From Pig to Human: Endo-Epicardial Substrate Characterization Using Dual Optical Mapping

Jimena Siles[1,3], Casey Lee-Trimble[3], Evan Rheaume[3], Flavio Fenton[3], João Salinet[1], Ilija Uzelac[2]

[1]HEartLab, Federal University of ABC, São Bernardo do Campo, Brazil
[2]School of Medicine, Virginia Commonwealth University, Richmond, VA, USA
[3]School of Physics, Georgia Institute of Technology, Atlanta, GA, USA

Abstract

Understanding the dissociation between endocardial and epicardial electrical activity is critical for investigating arrhythmia mechanisms. In this study, we used a dual optical mapping system to simultaneously record transmembrane voltage signals from both surfaces (endo-epi) in porcine and human hearts. Endocardium was paced at incrementally faster rates, starting with a pacing cycle length (PCL) of 1000 ms and continuing until conduction block or an arrhythmia. Porcine hearts showed an abrupt transition to fibrillation with negligible action potential duration (APD) alternans. In contrast, human hearts exhibited marked alternans and repolarization heterogeneity prior to fibrillation, with APD reaching up to 600 *ms in the endocardium at PCL=230 ms. During fibrillation, endocardial maps revealed areas of conduction block and multiple reentrant sites, whereas epicardial activation was slower compared with the endocardium. These results shows endo-epicardial dissociation and species-specific differences in arrhythmogenesis, supporting the use of dual-surface optical mapping as a tool for translational cardiac research.*

1. Introduction

Understanding the electrophysiological dissociation between the endocardium and epicardium is essential for uncovering the mechanisms involved in the initiation and maintenance of cardiac arrhythmias, as well as for the development of treatment strategies [1]. Although these ventricular layers are functionally interconnected, differences in activation and repolarization dynamics have been increasingly linked to arrhythmogenesis. Most prior studies, however, have examined each surface independently, limiting the assessment of spatiotemporal interactions that may drive complex arrhythmic behavior [2]. The use of porcine models is well established in cardiac research due to their anatomical and electrophysiological similarities to the human heart [3], thereby enabling meaningful translational comparisons between normal and pathological conditions. In this study, we employed a dual optical mapping system to simultaneously record high-resolution signals from both endocardial and epicardial surfaces in healthy porcine and diseased human hearts. By analyzing local activation time (LAT), APD, and restitution curves, we aimed to highlight the role of endo-epicardial dissociation in arrhythmia development. Furthermore, the investigation of electrophysiological differences under normal (healthy porcine hearts) and pathological conditions (diseased human hearts) reinforces the value of translational models in advancing future electrophysiological research and therapies.

2. Methods

2.1. Experimental Procedure

Three female porcine hearts (35–40 kg) were donated from a surgery training facility right after euthanasia as presented in previous studies [4]. Shortly euthanasia was performed using a pentobarbital and phenytoin solution. Then, pig hearts were quickly excised through left lateral thoracotomy and perfused right away with Tyrode solution (in mM: 123.00 NaCl, 4.50 KCl, 20.00 $NaHCO_3$, 4.78 $NaH_2PO_4.H_2O$, 2.09 $MgCl_2.6H_2O$, 11.00 glucose, and 1.80 $CaCl_2$). The human hearts were provided by the VCU Heart Transplant Program and approved by the VCU Institutional Review Board (IRB). Hearts were surgically extracted and perfused with ice-cold cardioplegic solution administered via both the left and right coronary arteries. Tyrode solution (in mM: 128.20 NaCl, 4.70 KCl, 25 $NaHCO_3$, 1.2 $NaH_2PO_4.H_2O$, 1.05 $MgCl_2.6H_2O$, 10 glucose, and 1.80 $CaCl_2$) was continuously perfused during the recordings. To enable dual-surface optical recordings, tissue preparations were mounted in a free wall preparation, which involved surgical exposure of both endocardial and epicardial right ventricle (RV) surfaces. Endocardium was paced at incrementally faster rates, starting with a PCL

of 1000 ms and continuing until conduction block or an arrhythmia.

2.2. Dual Optical Mapping System Implementation

Dual optical mapping was conducted at two institutions: Georgia Institute of Technology (GT, system 1), focusing primarily on porcine studies, and Virginia Commonwealth University (VCU, system 2), dedicated to human experiments. Image acquisition was performed using two high-speed cameras: one above the endocardium (CAM A), and the other placed on the side of the tank (CAM B), a mirror positioned at a 45-degree angle relative to the table helps to record the epicardium [5] (Fig. 1). CAM A and CAM B were equipped with fixed focal length lenses: 6 mm f/2.0 (DF6HA-1S) and Fujinon 12.5 mm f/1.4 (HF12.5HA-1B), respectively. Optical signals were passed through a dual-stage emission filter composed of a 595/40 nm bandpass filter and a 700 nm long-pass filter. Cameras in system 1 were EMCCD (Evolve 128, Photometrics) with a spatial resolution of 128 × 128 pixels, while system 2 used Pregius CMOS cameras (DMK 37BUX287) with a resolution of 720 × 540 pixels. Excitation source was provided by four red LEDs with a center wavelength of 660 nm, combined with a 660/10 nm bandpass filter (Edmund Optics). Both systems operated at a sampling frequency of 500 Hz. In both setups, the voltage-sensitive dye JPW-6003 was used for transmembrane potential recordings.

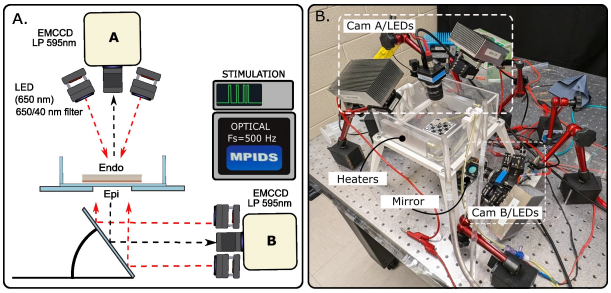

Figure 1. Dual optical mapping setup. (A) Optical cameras positioned above and below the tissue preparation, with the endocardial and epicardial sides illuminated by LEDs; (B) Real image of the setup with its components.

2.3. Signal Processing and Metric Extraction

The normalized change in fluorescence intensity, $\Delta F/F$, was calculated as $(F - F_0) / F_0$, where F_0 represents the fluorescence intensity of the polarized cell membrane and F that of the depolarized membrane [6]. Signals underwent baseline drift removal using a high-pass Butterworth filter with a cutoff frequency of 0.5 Hz. Subsequently, the signals were smoothed using a two-dimensional spatiotemporal Gaussian filter with a spatial kernel size of 11×11 and a temporal kernel size of 1×11 [6]. For this work we analyzed 2 metrics: LAT and APD, to study endo-epi differences trough the restitution curve and LAT maps. The optical LAT is calculated by linear fit (Polyfit Matlab function) along the OAP upstroke and determining the 50% rise of the OAP upstroke [7]. The APD was defined as the time point when the cell has repolarized to 80% (APD_{80}) from the maximum upslope of the action potential was detected, and the repolarization level was calculated as 80% of the distance from the peak back to the baseline level [8]. For the OAPs restitution curve, for each PCL, a segment of three beats was selected from sixteen points over the endocardium and epicardium (4 x 4 configuration). For each segment of three beats APD_n was calculated, and then subtracted from the PCL to obtain the diastolic interval (DI_n). The curve was calculated for two consecutive beats, as the relation between APD_{n+1} and DI_n [9].

3. Results

3.1. Signal Characterization

Figure 2 shows representative examples of the epicardial (top) and endocardial (bottom) surfaces of pig and human hearts, respectively.

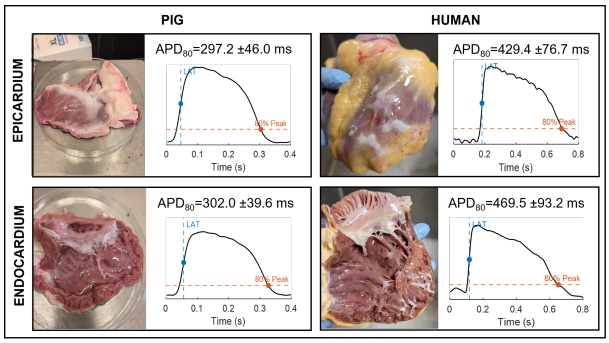

Figure 2. Anatomical characterization of pig and human hearts presenting the epicardium and endocardium sides and a representative optical action potential (PCL=800 ms) showing the determination of LAT, and APD_{80}.

Pig hearts had average dimensions of 11.7×9.5 cm (SD = 0.3 and 0.5 cm, respectively) and an average weight of 216.9 g (SD = 23.0 g). The human hearts had average dimensions of 17.0×12.7 cm (SD = 1.0 and 0.6 cm, respectively) and an average weight of 556.0 g (SD = 67.7 g). Human hearts displayed increased adipose thickness and, in certain cases, signs of fibrotic tissue.

For LAT and APD_{80} detection, a PCL of 800 ms was applied. Activation and repolarization timings were cal-

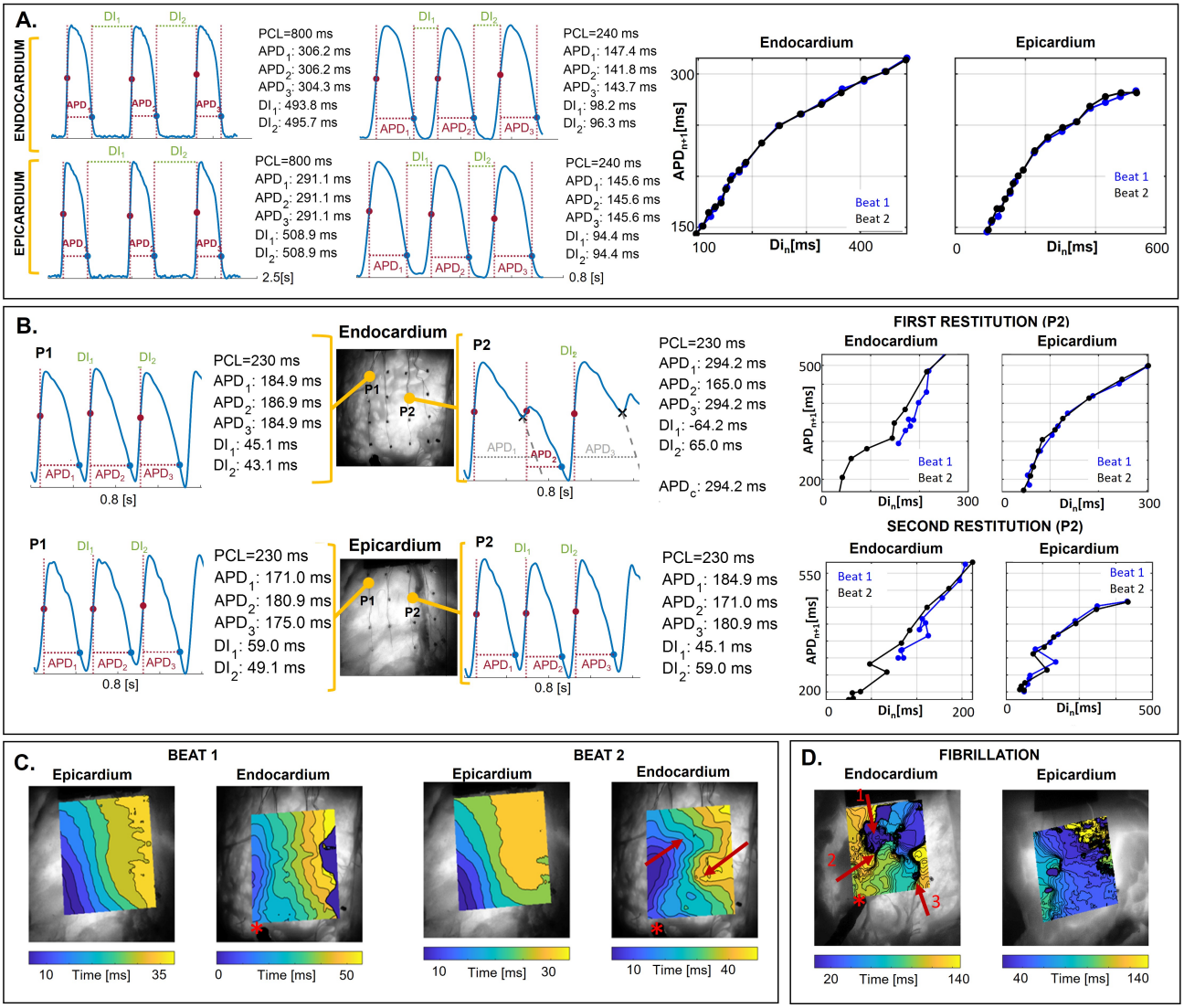

Figure 3. (A) OAPs displayed for PCLs of 800 and 240 ms. At right the endo and epi restitution curves for beat 1 (blue) and beat 2 (black); (B) OAP at P1 and P2 from a human heart PCL of 230 ms (top panel). Restitution curves at P2 during the first restitution and a second; (C) LAT optical maps from endocardium and epicardium of a human heart plotted at two consecutive beats (beat 1 and beat 2); (D) Endocardium an epicardium optical maps during fibrillation in human heart.

culated using three consecutive beats recorded simultaneously from 16 pixels. Figure 2 provides illustrative examples of OAPs acquired from the epicardium and endocardium of the RV in both pig and human hearts. LAT are marked by vertical blue dotted lines, whereas repolarization timings (represented by APD_{80}) are indicated by orange dotted lines. The mean APD_{80} for the pig epicardium was 297.2 ms (SD = 46.0 ms) and 302.0 ms (SD = 39.6 ms) for the endocardium, while for the human epicardium it was 429.4 ms (SD = 76.7 ms) and 469.5 ms (SD = 93.2 ms) for the endocardium. Figure 3A (left panel) presents representative OAPs acquired simultaneously from both sides of a pig heart at two PCLs: 800 ms and 240 ms. LATs are indicated by red circles, while the APD_{80} and DI intervals are highlighted by a blue circle and a dotted green line, respectively. Numerical values are summarized to the right of each plot. The restitution plots (right panel) shows the absence of alternans.

Figure 3B shows OAP recordings at P1 and P2 from the endocardium and epicardium of a human heart. At a PCL of 230 ms, APD_{80} values at P1 were approximately 185 ms (endocardium) and 175 ms (epicardium), with longer APD observed endocardially. At P2, APD alternans was evident, particularly in the endocardium, reaching approximately

600 ms. In some alternans episodes adjustment of APD termination was needed, as is presented with a dotted gray line in endocardium P2 at PCL of 230ms. First and second restitution curves further illustrate differences at P2.

3.2. Map Characterization

Figure 3C presents comparative activation maps obtained from simultaneous endocardial and epicardial optical recordings during Beat 1 and Beat 2 in a human heart, an asterisk (*) highlights the pacing spot. In Beat 1 (longer APD), both surfaces show synchronized activation. Notably, in Beat 2 (shorter APD), the endocardial map reveals fragmented activation patterns with multiple wavefront entries (red arrows), suggesting the early development of a potential reentrant circuit. Figure 3D shows LAT maps during ventricular fibrillation in a human heart, recorded from the endocardial (left) and epicardial (right) surfaces. The endocardial map shows the first activated areas (marked as 1), as well as two distinct sites of wavebreak or potential reentrant activity (2 and 3), suggestive of localized reentry. In contrast, the epicardial surface shows a less defined propagation pathways. These findings reveal marked endo-epicardial differences in the spatiotemporal dynamics of wavefront propagation during fibrillation.

4. Discussion and Conclusion

Using a dual optical mapping approach, we characterized endo-epicardial differences in healthy porcine and diseased human hearts. Porcine hearts served as a physiological reference, rapidly progressing to fibrillation with minimal APD alternans. In contrast, human hearts exhibited marked APD alternans, heterogeneous restitution, and conduction fragmentation prior to fibrillation more like in canine experiments [5]. Therefore, in relation to alternans, canine physiology may be closer to human than porcine. During arrhythmia, the endocardium showed conduction blocks and multiple reentrant sites, while epicardial activation was slower than endocardium [10]. These findings underscore the importance of transmural mapping to elucidate arrhythmogenic mechanisms and support the translational relevance of this dual-surface approach. Furthermore, they align with clinical evidence showing that spatial APD dispersion and alternans predict arrhythmia risk [5, 11].

Acknowledgments

This work was supported by FAPESP grants #2020/03601-9, #2023/04822-7, and #2018/25606-2, CNPq INCT INTERAS call 58/2022, NIH grant 2R01HL143450–05A1 and the Dr. Kenneth Ellenbogen Endowment. We thank the VCU surgeons for the explanted human hearts.

References

[1] Berruezo A, Fernández-Armenta J, Mont L, Zeljko H, Andreu D, Herczku C, Boussy T, Tolosana JM, Arbelo E, Brugada J. Combined endocardial and epicardial catheter ablation in arrhythmogenic right ventricular dysplasia incorporating scar dechanneling technique. Circulation Arrhythmia and Electrophysiology 2012;5(1):111–121.

[2] Darbar D, Olgin JE, Miller JM, Friedman PA. Localization of the origin of arrhythmias for ablation: From electrocardiography to advanced endocardial mapping systems. Journal of Cardiovascular Electrophysiology 2001; 12(11):1309–1325.

[3] Schüttler D, Bapat A, Kääb S, Lee K, Tomsits P, Clauss S, Hucker WJ. Animal models of atrial fibrillation. Circulation Research 2020;127(1):91–110.

[4] Uzelac I, Crowley CJ, Iravanian S, Kim TY, Cho HC, Fenton FH. Methodology for cross-talk elimination in simultaneous voltage and calcium optical mapping measurements with semasbestic wavelengths. Frontiers in Physiology 2022;13:812968.

[5] Gizzi A, Cherry EM, Gilmour Jr RF, Luther S, Filippi S, Fenton FH. Effects of pacing site and stimulation history on alternans dynamics and the development of complex spatiotemporal patterns in cardiac tissue. Frontiers in Physiology 2013;4:71.

[6] Uzelac I, Crowley CJ, Fenton FH. Isosbestic point in optical mapping; theoretical and experimental determination with di-4-anbdqpq transmembrane voltage sensitive dye. In 2019 Computing in Cardiology (CinC). IEEE, 2019; Page–1.

[7] Efimov IR, Nikolski VP, Salama G. Optical imaging of the heart. Circulation Research 2004;95(1):21–33.

[8] Stoks J, Bear LR, Vijgen J, Dendale P, Peeters R, Volders PG, Cluitmans MJ. Understanding repolarization in the intracardiac unipolar electrogram: a long-lasting controversy revisited. Frontiers in Physiology 2023;14:1158003.

[9] Guevara M, Ward G, Shrier A, Glass L. Electrical alternans and period doubling bifurcations. IEEE Comp Cardiol 1984;562:167–170.

[10] Fenton FH, Cherry EM, Gray RA, Hastings HM, Evans SJ. Fibrillation without alternans in porcine ventricles. Heart Rhythm 2005;2(5):S301–S302.

[11] Laurita KR, Rosenbaum DS. Cellular mechanisms of arrhythmogenic cardiac alternans. Progress in Biophysics and Molecular Biology 2008;97(2-3):332–347.

Address for correspondence:

Jimena Gabriela Siles Paredes
Federal University of ABC - UFABC
Street: Av. Anchieta, São Bernardo do Campo - SP, Brazil
E-mail: jimena.gabriela@ufabc.edu.br